

Polaronic trapping of electrons and holes by native defects in anatase TiO₂

Benjamin J. Morgan* and Graeme W. Watson†

School of Chemistry, Trinity College, University of Dublin, Dublin 2, Ireland

(Received 18 November 2009; published 16 December 2009)

We have investigated the formation of native defects in anatase TiO₂ using density functional theory (DFT) modified with on-site Coulomb terms (DFT+*U*) applied to both Ti *d* and O *p* states. Oxygen vacancies and titanium interstitials are found to be deep donors that trap two and four electrons, with transition levels that explain the two features seen in deep level transient spectroscopy experiments. Titanium vacancies are deep acceptors accommodating four holes. Self-trapping of both electrons and holes is also predicted. In all cases both donor and acceptor trap states correspond to strongly localized small polarons, in agreement with experimental EPR data. Variation in defect formation energies with stoichiometry explains the poor hole-trapping of reduced TiO₂.

DOI: 10.1103/PhysRevB.80.233102

PACS number(s): 71.38.Ht, 71.55.-i, 82.50.-m

In semiconductors used in photocatalysis and photovoltaics, the primary process is the light-induced production of charge carriers.¹ Photocatalysis proceeds by photoexcitation of electrons to unoccupied bands, producing free electron-hole pairs. These charge carriers then typically undergo trapping, followed by diffusion to the surface where they can initiate reactions of adsorbed molecules. Electron-hole recombination is often a major competing process, and it is highly desirable to promote charge separation and inhibit subsequent charge-carrier-recombination in order to improve the quantum efficiency of photocatalytic processes.

TiO₂ has been widely studied as a photocatalyst for the degradation of environmental pollutants,¹ and for water splitting.² Nanocrystalline anatase TiO₂ is often used, since it is more photocatalytically active than the ground-state polymorph, rutile, and the diffusion pathways of photogenerated charge carriers to the surface are shortened, resulting in increased quantum efficiencies.

Following photoexcitation, trapping of charge carriers occurs on a nanosecond time scale.³ Defects are thought to play a critical role in the trapping process by acting as recombination centers. For example, *n*-type doping of anatase reduces the photocatalytic activity of experimental samples,⁴ and reduced anatase is less efficient than stoichiometric TiO₂ in the trapping of photogenerated holes.⁵ Understanding the interaction of defects with charge carriers is essential for the optimization of TiO₂ samples for photocatalysis. Electron- and hole traps have both been observed in EPR spectra.⁵⁻⁸ These data have been interpreted as charge localization at single atoms to give small polarons: hole trapping has been associated with O⁻ sites; O_O[•], and electron trapping with Ti³⁺ species; Ti_{Ti}[•]. Additional evidence for charge localization at Ti³⁺ states in *n*-type TiO₂ comes from core-level XPS shifts, and characteristic gap-state features observable in UPS spectra, with samples annealed to produce oxygen vacancies giving identical EPR signals to those seen following uv irradiation. Deep traps 0.9 and 0.5 eV below the conduction band edge have also been identified with deep level transient spectroscopy (DLTS).⁹

Na-Phattalung *et al.* have previously reported local density approximation (LDA)-density functional theory (DFT) calculations that predicted that both the oxygen vacancy (*V*_O)

and titanium interstitial (Ti_i) are shallow donors, and the titanium vacancy (*V*_{Ti}) is a shallow acceptor, with associated defect states corresponding to metallic bands at the valence and conduction band edges.¹⁰ Osorio-Guillén *et al.* used generalized gradient approximation (GGA)-DFT with *a posteriori* band-gap corrections, and in contrast reported deep donor levels for *V*_O and Ti_i, with the associated defect states at the bottom of the conduction band.¹¹ The prediction of delocalized defect states, however, is inconsistent with the localized polaronic description from experimental data.⁵⁻⁸

The failure of LDA and GGA DFT functionals to be unable to correctly describe defect states is well known for a number of wide-gap oxides.¹²⁻¹⁵ This is due to the self-interaction error (SIE) inherent to such functionals, which results in an artificial bias toward delocalization of partially occupied states.¹⁶ This problem is acute for localized metal *d* and *f* states, and also exhibited for oxygen *p* states.^{12,15} For TiO₂ it has been shown that experimental features of excess electron states that accompany *n*-type doping are only reproduced when the self-interaction error is corrected for.¹⁷⁻²² The need for self-interaction corrections in describing the polaronic nature of excess electrons and holes in TiO₂ has also been discussed by Deskins *et al.*^{23,24}

In this Brief Report we report a DFT+*U* examination of the transition levels and single particle levels of *n*- and *p*-type native defects in anatase TiO₂. In order to correctly describe these states we apply +*U* corrections to both Ti *d* and O *p* states. DFT+*U*{Ti_{*d*}} has been demonstrated to be suitable for *n*-type defects in TiO₂, yet no calculations to date have addressed the problem of the self-interaction error (SIE) for O-derived defect states. Using an *ab initio* *U*{O_{*p*}} value that correctly places the unoccupied O *2p* states relative to the valence band edge, we find that: *V*_O and Ti_i are deep donors, with the neutral defects producing single particle levels in the band gap; *V*_{Ti} is a quadruple deep donor, again with single particle levels in the band gap; both electrons and holes are predicted to undergo self-trapping; defect states for both native defects and self-trapped charge carriers correspond to holes or electrons trapped as small polarons to give O_O[•] and Ti_{Ti}[•].

Method. To counteract the problems associated with the SIE inherent to standard density functionals we have used

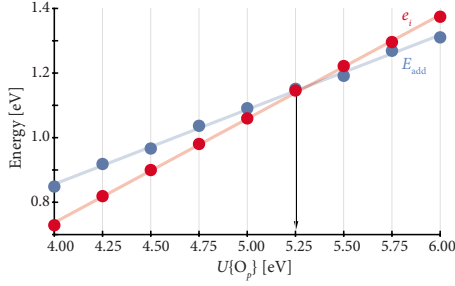


FIG. 1. (Color online) The electron addition energy, $E_{\text{add}} = E_{N+1} - E_N$, and the hole state eigenvalue (relative to the VBM) of the +1 charge state of anatase TiO_2 . The arrow shows the value of $U(\text{O}_p)$ for which Eq. (1) is satisfied.

the Perdew-Burke-Ernzerhof GGA functional,²⁵ supplemented with Dudarev on-site Hubbard corrections applied to both Ti d and O p states; DFT+ $U\{\text{Ti}_d, \text{O}_p\}$.²⁶ $U\{\text{Ti}_d\}$ was 4.2 eV, which gives the correct splitting between occupied and unoccupied Ti d states for O vacancies at the rutile TiO_2 (110) surface,¹⁸ and has been used to model both native n -type defects, and $\{\text{Nb}, \text{Ta}\}$ -doping of anatase TiO_2 .^{21,22} An *ab initio* $U\{\text{O}_p\}$ value of 5.25 eV was used, as described below. Calculations were performed in VASP (Refs. 27 and 28) with a plane-wave basis cutoff of 500 eV. Structures were relaxed until the forces on all atoms were less than $0.01 \text{ eV } \text{\AA}^{-1}$. Interactions between core and valence electrons were described using the projector augmented-wave method.²⁹ Calculations were performed using $3 \times 3 \times 1$ supercells (108 atoms) for all defects, except for the titanium vacancy, where $3 \times 3 \times 2$ supercells (216 atoms) were required to minimize interactions along the c direction. Γ -centered $2 \times 2 \times 2$ k -point sampling was used for all calculations. All calculations were spin polarized.

To determine $U\{\text{O}_p\}$ we used the *ab initio* fitting procedure of Lany and Zunger.¹⁵ For the (unknown) exact density functional the change in energy of the system when part of an electron is added or removed is linear.¹⁶ For addition of an electron to a hole state, this condition requires that

$$E(N+1) - E(N) = e_i(N). \quad (1)$$

Here $E(N+1) - E(N)$ is the electron addition energy, i.e., the difference in energy between the system with a self-trapped hole present (the +1 charge state), and the neutral system; where both are calculated at the optimized geometry for the hole system; and $e_i(N)$ is the eigenvalue of the hole state relative to the valence band maximum. Figure 1 shows the variation in $[E(N+1) - E(N)]$ and $e_i(N)$ for the +1 charge state of stoichiometric anatase TiO_2 . Equation (1) is satisfied for $U\{\text{O}_p\} = 5.25 \text{ eV}$, giving the correct splitting between occupied and unoccupied O $2p$ states. The formation enthalpy of a defect with charge state q is given by

$$\Delta H_f(D, q) = (E^{D, q} - E^H) + \sum_i n_i (E_i + \mu_i) + q E_F, \quad (2a)$$

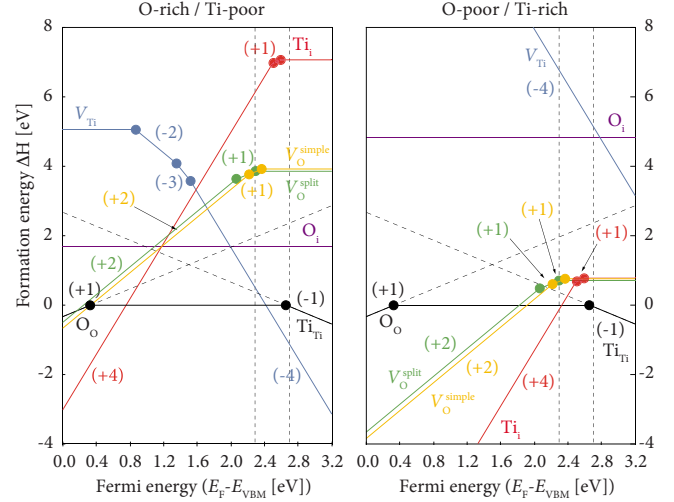


FIG. 2. (Color online) Formation energies for intrinsic defects in anatase TiO_2 . The solid dots denote transition levels $\epsilon(q/q')$. The diagonal dashed lines give the energies of metastable self-trapped electrons and holes produced by photoexcitation. The vertical dashed lines are the DLTS levels reported by Miyagi *et al.*⁹

$$\text{where } E_F = \Delta E_F + \epsilon_{\text{VBM}}^H + \Delta v(D). \quad (2b)$$

E^H is the total energy of the stoichiometric host supercell and $E^{D, q}$ is the total energy of the defective cell. Elemental reference energies, E_i , were obtained from calculation on the constituent elements in their standard states, i.e., $\text{O}_{2(\text{g})}$ and $\text{Ti}_{(\text{s})}$. n_α is the number of atoms transferred to or from reservoirs with respective chemical potentials μ_α . These chemical potentials represent specific equilibrium growth conditions, within the general constraint of the formation enthalpy of anatase TiO_2 : $\mu_{\text{Ti}} + 2\mu_{\text{O}} = \Delta H_f^{\text{TiO}_2} = -8.11 \text{ eV}$. The upper limit for $\mu(\text{O})$ is governed by the formation of $\text{O}_{2(\text{g})}$; $\mu(\text{O}) = 0 \text{ eV}$ and $\mu(\text{Ti}) = -8.11 \text{ eV}$. The O-poor/Ti-rich lower limit to $\mu(\text{O})$ is constrained by the formation of Ti_2O_3 ; $2\mu(\text{Ti}) + 3\mu(\text{O}) \leq \Delta H_f^{\text{Ti}_2\text{O}_3} = -13.08 \text{ eV}$, which gives $\mu(\text{O}) = -3.14 \text{ eV}$; $\mu(\text{Ti}) = -1.82 \text{ eV}$. ΔE_F can range from the VBM ($E_F = 0 \text{ eV}$) to the CBM ($E_F = 3.2 \text{ eV}$). ϵ_{VBM}^H is the energy of the VBM in the stoichiometric system, and $\Delta v(D)$ is a core-level alignment between the stoichiometric and defect cells, obtained by taking the difference of O $1s$ core-level energies for an oxygen atom well removed from the defect position. Thermodynamic ionization (transition) levels, $\epsilon_D(q/q')$, are given by the Fermi energy at which the energies of two charge states, q and q' , of the defect D are equal;

$$\epsilon_D(q/q') = \frac{\Delta H_f(D, q) - \Delta H_f(D, q')}{q' - q}. \quad (3)$$

Results. Fig. 2 shows calculated formation energies and transition levels for Ti_{Ti} , V_{O} , O_i , and V_{Ti} . Oxygen vacancy data are presented for both the “simple” V_{O} ; where the excess electrons are localized at the two Ti sites neighboring the vacancy; and for the “split” V_{O} ; where one electron is localized at a next-nearest Ti site.²¹ Also shown are the calculated

TABLE I. Single particle levels relative to the valence band maximum in eV. For the defects with occupied levels, the conduction band offset at the Γ point is given in brackets.

V_O^{simple}		V_O^{split}		Ti_i				V_{Ti}				Ti_{Ti}	O_O
0	+1	0	+1	0	+1	+2	+3	0	-1	-2	-3	-1	+1
				1.88 (0.74)				1.91					
				1.64 (0.98)	1.62 (1.00)			1.76	1.86				
1.47 (1.15)		1.35 (1.27)		1.32 (1.30)	1.45 (1.17)	1.53 (1.09)		1.76	1.60	1.90			
1.14 (1.48)	1.27 (1.35)	1.26 (1.36)	1.25 (1.37)	0.88 (1.74)	0.88 (1.74)	0.88 (1.73)	0.91 (1.71)	1.53	1.48	1.60	1.64	1.80	1.09

energies for self-trapped holes, O_O^\bullet and electrons, Ti_{Ti}' . Ti_i and V_O have deep transition levels, as predicted by Osorio-Guillén *et al.*¹¹ The single particle levels associated with the neutral and intermediate-charge defects are in the band gap; Table I and Fig. 3; in contrast to previous calculations.^{10,11} These deep states correspond to electrons trapped at Ti sites as small polarons. For the neutral V_O two electrons are close to the vacancy site, whereas for Ti_i one electron associated with the deepest level ~ 1.72 eV below the CBM is trapped at the interstitial Ti site, and the other three are localized at lattice Ti sites neighboring to the interstitial, giving $[Ti_i^{\bullet\bullet\bullet} + 3Ti_{Ti}']$.²¹

The transition levels for V_{Ti} are also within the band gap. The single particle levels for these hole states are well separated from the VBM, and correspond to small polarons at up to four of the six O sites surrounding the vacancy; Fig. 4. Such trapping of holes at individual defect site ligands is well known for a range of wide-gap oxides,^{30,31} and polaronic binding of holes has been predicted for Al-doped TiO_2 .³² For the neutral vacancy the four holes are localized at two equatorial and two apical sites of the distorted octahedron around the vacancy site. As the Fermi level is increased, the apical sites are detrapped first, producing well separated $\epsilon(0/-2)$ and $\{\epsilon(-2/-3), \epsilon(-3/-4)\}$ transition levels. O_i is present as a peroxide ion at an oxygen lattice site, giving $(O_2)_O^\times$, as described by Na-Phattalung *et al.*¹⁰ Since this defect neither donates nor accepts charge carriers its

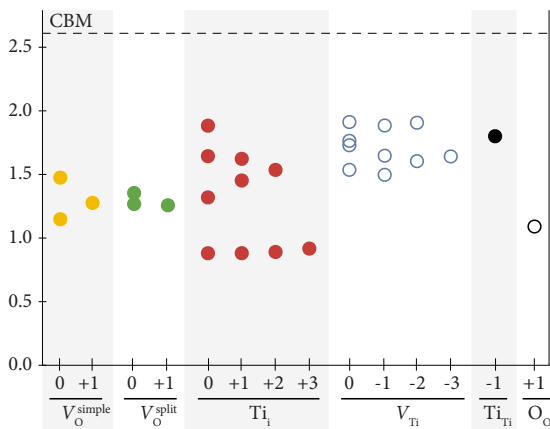


FIG. 3. (Color online) Single particle levels for all defect states showing levels in the band gap. Filled circles are occupied levels due to n -type defects, and empty circles are unoccupied levels due to p -type defects.

presence is expected to have little effect on the photochemistry of the material.

Both electrons and holes are also predicted to undergo self-trapping. Self-trapped electrons correspond to strongly localized polaronic states at single Ti centers; Ti_{Ti}' ; and self-trapped holes are similarly strongly localized at single O centers; O_O^\bullet . The energy of a self-trapped photogenerated electron-hole pair is 2.35 eV.³³ The localized nature of the defect states is in agreement with the experimental EPR data,⁵ in contrast to previous LDA/GGA studies.^{10,11}

Miyagi *et al.* have reported DLTS data for anatase TiO_2 thin films showing deep trap levels 0.5 and 0.9 eV below the conduction band edge, with the trap at 0.9 eV present at a greater concentration.⁹ Our calculated $\epsilon(0/+1)$ transition levels for Ti_{Ti} and V_O^{simple} are 0.60 and 0.91 eV from the experimental CBM of 3.2 eV, leading us to assign the trap at 0.5 eV to Ti_{Ti} , and the trap at 0.9 eV to V_O ; Fig. 2.

The calculated defect formation energies for O-rich/Ti-poor conditions are consistent with the known formation of charge-compensating V_{Ti} when TiO_2 is doped n -type (with, e.g., Nb) under ambient oxygen partial pressures.^{34,35} The variation in defect formation energies with sample composition also explains the reported absence of an EPR signal for photogenerated holes in reduced TiO_2 .⁵ Under O-poor/Ti-rich conditions oxygen vacancies and titanium interstitials form easily, whereas the formation energy of compensating V_{Ti} is very high. Hence the Fermi level is high in the band gap, and neutral oxygen vacancies and titanium interstitials, or even self-trapped electrons, will be present at high concentrations, and will act as recombination centers.

Summary. We have used DFT+ U with on-site Coulomb

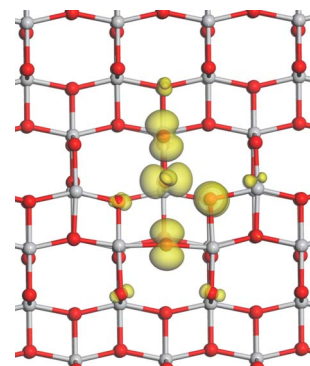


FIG. 4. (Color online) Spin density for the Ti vacancy defect state in anatase TiO_2 . The charge isosurface is shown at $0.05 \text{ e } \text{\AA}^{-3}$.

corrections for both Ti *d* and O *p* states to study the native defects of anatase TiO₂. This corrects for the self-interaction error of *n*- and *p*-type defect states, and predicts that V_O, Ti_{Ti}, and V_{Ti} are characterized by strongly localized electrons or holes, in agreement with experimental EPR data. We find that transition levels for these defects are deep, and assign the DLTS signals at 0.9 and 0.5 eV to V_O and Ti_{Ti}, respectively. Calculated formation energies allow the experimentally observed variation in photo-hole lifetimes with stoichi-

ometry to be understood in terms of the number of “hole-killer” *n*-type electron traps present.

This research was supported by Science Foundation Ireland under Grant No. 06/IN/1/192, and supplement 06/IN/1/192/EC07. Calculations were performed on the IITAC supercomputer as maintained by the Trinity Centre for High Performance Computing (TCHPC), and the Stokes supercomputer; maintained by the Irish Centre for High-End Computing (ICHEC).

*morganb@tcd.ie

†watsong@tcd.ie

- ¹A. L. Linsebigler, G. Lu, and J. T. Yates, Jr., *Chem. Rev.* **95**, 735 (1995).
- ²A. Fujishima and K. Honda, *Nature* **238**, 37 (1972).
- ³D. P. Colombo and R. M. Bowman, *J. Phys. Chem.* **99**, 11752 (1995).
- ⁴T. Miyagi, M. Kamei, I. Sakaguchi, T. Misuhashi, and A. Yamzaki, *Jpn. J. Appl. Phys.* **43**, 775 (2004).
- ⁵T. Berger, M. Sterrer, O. Diwald, E. Knözinger, D. Panayotov, T. L. Thompson, and J. T. Yates, Jr., *J. Phys. Chem. B* **109**, 6061 (2005).
- ⁶R. F. Howe and M. Grätzel, *J. Phys. Chem.* **91**, 3906 (1987).
- ⁷S. Zhou, A. Čížmar, K. Potzger, M. Krause, G. Talut, M. Helm, J. Fassbender, S. A. Zvyagin, J. Wosnitza, and H. Schmidt, *Phys. Rev. B* **79**, 113201 (2009).
- ⁸S. Yang, L. E. Halliburton, A. Manivannan, P. H. Bunton, D. B. Baker, M. Klemm, S. Horn, and A. Fujishima, *Appl. Phys. Lett.* **94**, 162114 (2009).
- ⁹T. Miyagi, M. Kamei, T. Mitsushashi, and A. Yamazaki, *Appl. Phys. Lett.* **83**, 1782 (2003).
- ¹⁰S. Na-Phattalung, M. F. Smith, K. Kim, M.-H. Du, S.-H. Wei, S. B. Zhang, and S. Limpijumnong, *Phys. Rev. B* **73**, 125205 (2006).
- ¹¹J. Osorio-Guillén, S. Lany, and A. Zunger, *Phys. Rev. Lett.* **100**, 036601 (2008).
- ¹²M. Nolan and G. W. Watson, *J. Chem. Phys.* **125**, 144701 (2006).
- ¹³D. O. Scanlon, A. Walsh, B. J. Morgan, M. Nolan, J. Fearon, and G. W. Watson, *J. Phys. Chem. C* **111**, 7971 (2007).
- ¹⁴D. O. Scanlon, B. J. Morgan, G. W. Watson, and A. Walsh, *Phys. Rev. Lett.* **103**, 096405 (2009).
- ¹⁵S. Lany and A. Zunger, *Phys. Rev. B* **80**, 085202 (2009).
- ¹⁶P. Mori-Sánchez, A. J. Cohen, and W. Yang, *Phys. Rev. Lett.* **100**, 146401 (2008).
- ¹⁷C. Di Valentin, G. Pacchioni, and A. Selloni, *Phys. Rev. Lett.* **97**, 166803 (2006).
- ¹⁸B. J. Morgan and G. W. Watson, *Surf. Sci.* **601**, 5034 (2007).
- ¹⁹C. J. Calzado, N. C. Hernández, and J. F. Sanz, *Phys. Rev. B* **77**, 045118 (2008).
- ²⁰C. Di Valentin, G. Pacchioni, and A. Selloni, *J. Phys. Chem. C* **113**, 20543 (2009).
- ²¹B. J. Morgan and G. W. Watson, *J. Phys. Chem. C* (to be published).
- ²²B. J. Morgan, D. O. Scanlon, and G. W. Watson, *J. Mater. Chem.* **19**, 5175 (2009).
- ²³N. A. Deskins and M. Dupuis, *Phys. Rev. B* **75**, 195212 (2007).
- ²⁴N. A. Deskins and M. Dupuis, *J. Phys. Chem. C* **113**, 346 (2009).
- ²⁵J. P. Perdew, K. Burke, and M. Ernzerhof, *Phys. Rev. Lett.* **77**, 3865 (1996).
- ²⁶S. L. Dudarev, G. A. Botton, S. Y. Savrasov, C. J. Humphreys, and A. P. Sutton, *Phys. Rev. B* **57**, 1505 (1998).
- ²⁷G. Kresse and J. Hafner, *Phys. Rev. B* **49**, 14251 (1994).
- ²⁸G. Kresse and J. Furthmüller, *Comput. Mater. Sci.* **6**, 15 (1996).
- ²⁹P. E. Blöchl, *Phys. Rev. B* **50**, 17953 (1994).
- ³⁰O. F. Schirmer, *J. Phys.: Condens. Matter* **18**, R667 (2006).
- ³¹A. M. Stoneham, J. Gavartin, A. L. Shluger, A. V. Kimmel, D. M. Ramo, H. M. Ronnow, G. Aeppli, and C. Renner, *J. Phys.: Condens. Matter* **19**, 255208 (2007).
- ³²A. Stashans and S. Bermeo, *Chem. Phys.* **363**, 100 (2009).
- ³³In general, the self-energy of small polarons includes contributions due to lattice fluctuations that can be expressed as non-adiabatic tunneling terms [J. T. Devreese and A. S. Alexandrov, *Rep. Prog. Phys.* **72**, 066501 (2009)]. Since the defect structures correspond to optimization at 0 K, any vibrational motion is “frozen out” and the self-energies presented here correspond to the adiabatic limit.
- ³⁴J. F. Baumard and E. Tani, *J. Chem. Phys.* **67**, 857 (1977).
- ³⁵S. Zhang, S. B. Ogale, W. Yu, X. Gao, T. Liu, S. Ghosh, G. P. Das, A. T. S. Wee, R. L. Greene, and T. Venkatesan, *Adv. Mater.* **21**, 2282 (2009).